Hindawi
Shock and Vibration
Volume 2019, Article ID 6410362, 11 pages
https://doi.org/10.1155/2019/6410362

Research Article

Dynamic Shear Properties of Recycled Waste Steel Slag Used as a Geo-Backfill Material

Liyan Wang[1], **Jiatao Yan**[2], **Qi Wang**[2], **Binghui Wang**[2] and **Wenxue Gong**[3]

[1]*Professor (Ph D), School of Civil and Architectural Engineering, Jiangsu University of Science and Technology, No. 2 Mengxi Road, Zhenjiang, Jiangsu Province, China*
[2]*Master Student (Ba.), School of Civil and Architectural Engineering, Jiangsu University of Science and Technology, No. 2 Mengxi Road, Zhenjiang, Jiangsu Province, China*
[3]*Associate Professor (Ph D), School of Civil and Architectural Engineering, Jiangsu University of Science and Technology, No. 2 Mengxi Road, Zhenjiang, Jiangsu Province, China*

Correspondence should be addressed to Liyan Wang; wly_yzu@163.com

Received 15 July 2018; Revised 24 November 2018; Accepted 22 April 2019; Published 2 June 2019

Academic Editor: Giuseppe Petrone

Waste steel slag is a recycled industrial solid waste and is sometimes used as backfills, but the dynamic shear properties of waste steel slag have not been researched at present. To understand the dynamic shear properties of waste steel slag, the resonance column tests were carried out to investigate the dynamic shear modulus and damping ratio of the steel slag considering the effect of the relative density of steel slag and confining pressure. The maximum dynamic shear modulus was discussed, and the dynamic model of the steel slag was constructed by the Hardin–Drnevich model. The regression analysis of the normalized dynamic shear modulus ratio and damping ratio of the steel slag showed that the dynamic model was very fit for the steel slag. The comparisons of the dynamic shear properties of the steel slag with those of Nanjing fine sand and Fujian standard sand showed that the steel slag had similar dynamic shear resistance to Fujian standard sand and had potential to become a substitute for sand in the practical geotechnical engineering in the future.

1. Introduction

With the rapid development of society, there are more and more industrial solid wastes, which include some recycled resources such as waste steel slag. Steel slag is a by-product of the steelmaking process, and the annual output increases continuously with the increase of the steel output. It is the second largest waste in metallurgical industry. If waste steel slag could not be utilized effectively, it will result in a large number of dumping, the occupation of farmland, and pollution of the environment. The discarded steel slag is shown in Figure 1. Recycled study on industrial solid wastes in civil engineering has recently become a new trend in the world, and the application of the four kinds of industrial wastes in Britain in asphalt pavement was summed up including waste slag [1]. Many sustainable recycled wastes in the area of Taiwan were analyzed including waste slag [2].

Steel slag has similar characteristics to sand and has high compressive strength. After eight-month aging, the performance of steel slag has been basically stable, and aged steel slag can be used as a kind of shallow-layer backfill material. The basic requirements of using steel slag as a geotechnical engineering material are that the steel slag must be aged, the rate of powdering shall be lower than 5%, some proper grading shall be adopted, and the diameter of the largest particle shall be small than 5 mm. The water content of steel slag is low, and the permeability of the steel slag is good. According to our research, the permeability coefficient is in the range of 10^{-3}~10^{-2}. The content of Fe_2O_3 in the waste steel slag sample is very low. Therefore, the aged waste steel slag would not rust over time and would not be reacted with water.

Steel slag pile was initially applied to composite foundation [3], which showed steel slag was superior to the traditional gravel pile foundation in technical, economic, and social

Figure 1: Tested steel slag.

benefits. A mixture of steel slag and lime soil was formed and had good frost resistance and corrosion resistance. After compaction, the strength index even reached concrete strength [4]. Main influence factors of the expansion and powder of steel slag included maximum particle size, porosity, and free calcium oxide content [5] Steel slag was mixed into graded crushed stone subbase to make the foundation form a good early strength and higher shear resistance [6]. Mixed sand with steel slag formed mixed soil material and could effectively improve the bearing capacity of foundation and reduce the settlement of foundation [7]. The deformation and strength characteristics of lightweight soil mixed with waste steel slag and foamed plastics were studied by considering the influence of the steel slag mixing ratio and curing age [8].

The expansive soil by mixing the steel slag of 10%~20% was studied, and some conclusions were achieved that the steel slag could significantly reduce the expansion rate, liquid limit, and plastic index of expansive soil, and that the steel slag of 10%~20% could improve particle distribution and strength characteristics of expansive soil [9]. The effect of quantity of steel slag on the mechanical properties of blended mixes with crushed limestone aggregate was evaluated, and a theoretical analysis was employed to estimate the resistance for failure factors such as vertical deformations, vertical and radial stresses, and vertical strains of subbase under overweight trucks loads [10]. The results indicated that the mechanical characteristics and the resistance factors were improved by adding steel slag to the crushed limestone. Blast furnace slag in the granulated form was applied as a granular fill overlay on soft subgrade soil [11]. Stainless steel reducing slag (SSRS) in production of the soil-based controlled low-strength material (CLSM) was used as a cement substitute. Testing results indicate that SSRS with the specific surface area of 4551 cm^2/g can substitute for Portland cement up to 30% in production of excavated CLSM. Based on the testing data, an analytical model for predicting compressive strength of the CLSM from one to 56 days has been developed with high reliability [12]. The waste slag was applied into the underground deep wall method [13]. The carpet waste fibers and steel slag as environmental friendly additives were applied to overcome the swelling and weakness of the expansive soil [14]. The results showed that both chemical modification and mechanical reinforcement by adding fibers and slag are efficient methods to improve general properties of expansive clayey soil. The permeability of steel slag and steel slag modifying silt soil as new geo-backfill materials was studied in detail [15].

According to the above literature review, at present, the dynamic shear resistance characteristics of waste steel slag as a geo-backfill material have not been studied. Recently, many researches were carried out on dynamic shear properties of soils or soils mixed with other solid waste [16–22]. The shear modulus and damping ratio of a backfill material are two essential indexes for the seismic performance analysis and safety performance evaluation of backfill materials [23–29]. Dynamic properties of steel slag improved with sand-tire shreds admixture had been studied [30]. In this paper, the dynamic shear modulus and damping ratio of waste steel slag would be investigated by resonance column tests.

2. Experimental Work

2.1. Test Material. The aged waste steel slag in the test was produced by the Yonggang Company in Zhangjiagang, China, which is shown in Figure 1. The chemical composition of the waste steel slag is shown in Table 1. The content of free calcium oxide was 3.2% and less than 5%, and the ignition loss was 7.8% and less than 8% [31], which showed that the waste steel slag could be applied in geotechnical backfill.

The grain size distribution of the waste steel slag is shown in Figure 2. The bulk density of the waste steel slag was approximately 2.2 g/cm^3. The gradation characteristics of the steel slag are as follows: $d_{60} = 1.0$ mm, $d_{30} = 0.47$ mm, and $d_{10} = 0.12$ mm; the coefficient of uniformity (C_u) was 8.3, and the coefficient of curvature was 1.8 (C_c). Therefore, the steel slag was classified as the well-graded material.

2.2. Test Method. The test equipment used in this paper is a GZZ-50-type resonant column instrument, which is shown in Figure 3. According to the basic principle of the resonant column, the equipment could test dynamic shear strain (γ), dynamic shear modulus (G), and damping ratio (λ) of soil by the method of torsion vibration. The test sample size is 50 mm ($\varnothing$) × 100 mm (H). The instrument can be used to study the dynamic properties of unbroken samples in a small shear strain range of 10^{-6}~10^{-4}.

In the resonance column test, the main influence factors of the dynamic shear behavior of steel slag include relative density (D_r) and confining pressure (σ). In order to study the relationship between the relative density of steel slag and its dynamic shear characteristics, the resonant column tests of the steel slag samples with different relative densities were carried out. Samples were prepared according to *Geotechnical Test Method Standard* [3]. The maximum dry density is determined by the vibration hammer method, and the minimum dry density is determined by the funnel and cylinder method. The maximum dry density and the minimum dry density of the steel slag were, respectively, 2.58 g/cm^3 and 1.96 g/cm^3.

Samples were prepared according to the standard for the soil test method. The quality of the single sample was calculated according to the relative density of the steel slag. The relationship between the control density and the relative density can be expressed as follows:

Table 1: Chemical composition of waste steel slag in the test.

Composition	SiO_2	CaO	MgO	Fe_2O_3	Al_2O_3
Content α (%)	11.28	48.00	4.86	5.24	11.38
Composition	Na_2O	K_2O	Alkali content	f-CaO	Ignition loss
Content α (%)	0.06	0.08	0.11	3.2	7.8

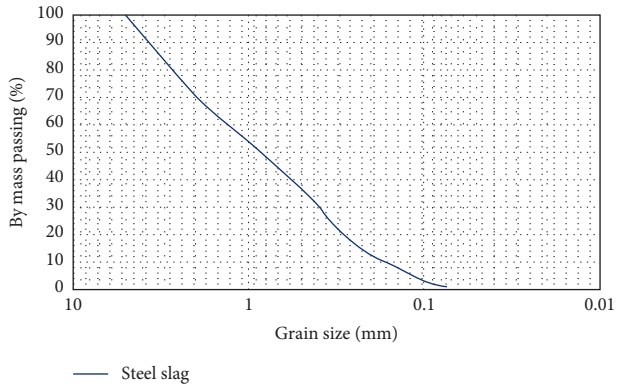

Figure 2: Grain distribution of test steel slag.

Figure 3: Resonant column apparatus (GZZ-50).

$$\rho_d = \frac{\rho_{dmax}\rho_{dmin}}{\rho_{dmax} - D_r(\rho_{dmax} - \rho_{dmin})}, \quad (1)$$

where D_r, ρ_{max}, ρ_{min}, and ρ_d represent the relative density, the maximum dry density, the minimum dry density, and the control density, respectively.

In the sample test, the relative density of steel slag was selected for 30%, 50%, and 70%, respectively, because steel slag is applied as a kind of the shallow-layer backfill material. The steel slag with a water content of 6% is thought in a natural state. Furthermore, when the water content is 6%, the steel slag is apt to form the test sample. Therefore, the water content in the test sample was set as 6%. The loading density (ρ) was calculated using the following equation:

$$\rho = \rho_d(1 + w), \quad (2)$$

where ω represents the water content of steel slag. The specific test parameters are shown in Table 2. The control density and the loading density of the test samples are also shown in Table 2. GZ1~GZ3, respectively, represent the test sample with the relative density of 30%, 50%, and 70%.

Table 2: Test schemes.

Sample number	Confining pressure σ (kPa)	Relative density D_r	Control density ρ_d (g/cm^3)	Water content ω (%)	Loading density ρ (g/cm^3)
GZ1	100, 200, 300	30%	2.11	6	2.24
GZ2	100, 200, 300	50%	2.23	6	2.36
GZ3	100, 200, 300	70%	2.36	6	2.50

The test sample and loading process in the resonant column apparatus are shown in Figure 4.

3. Results and Discussion

3.1. Effect of Relative Density. The relationships between the dynamic shear modulus (G) and the shear strain (γ) of the steel slag with different relative densities are shown in Figure 5 when the confining pressures (σ) were, respectively, 100 kPa, 200 kPa, and 300 kPa. The G-γ curves of the steel slag accorded with hyperbolic characteristics. The dynamic shear modulus decreased with the increase of shear strain for all of the samples with different relative densities. When the shear strain was small and in the range of $1 \times 10^{-6} < \gamma < 1 \times 10^{-5}$, the dynamic shear modulus of the steel slag decreased with the increase of the shear strain of the steel slag, but the magnitude of the decrease was small. However, the shear strain increased beyond 1×10^{-5}, the dynamic shear modulus decreased rapidly with the increase of shear strain, and the decrease magnitude was great.

The greater the relative density of the steel slag is, the larger the dynamic shear modulus of the steel slag is, and the overall relationships between dynamic shear modulus and shear strain were upward with the increase of the relative density of the steel slag. The relationship between the maximum dynamic shear modulus (G_{max}) and different relative densities is shown in Figure 6 when the confining pressure was 200 kPa. The maximum dynamic shear modulus of the steel slag increased with the increase of the relative density of steel slag. When the relative density of the steel slag was 70%, the maximum dynamic shear modulus of the steel slag was the maximum.

The relationships between the damping ratio (λ) and the shear strain of the steel slag with different relative densities are shown in Figure 7 when the confining pressures were 100 kPa, 200 kPa, and 300 kPa, respectively.

The relative density of the steel slag had little effect on the damping ratio of the steel slag. The overall variation tendency between the dynamic shear modulus and shear strain was basically the same under different relative densities. They were staggered and had nearly no offset.

When the shear strain was small and in the range of $1 \times 10^{-6} < \gamma < 1 \times 10^{-5}$, the damping ratio of the steel slag increased with the increase of shear strain, but the increase in magnitude was small. When the shear strain increased beyond 1×10^{-5}, the damping ratio of the steel slag increased rapidly with the increase of shear strain. The reason for this phenomenon was that the steel slag was in an elastic state

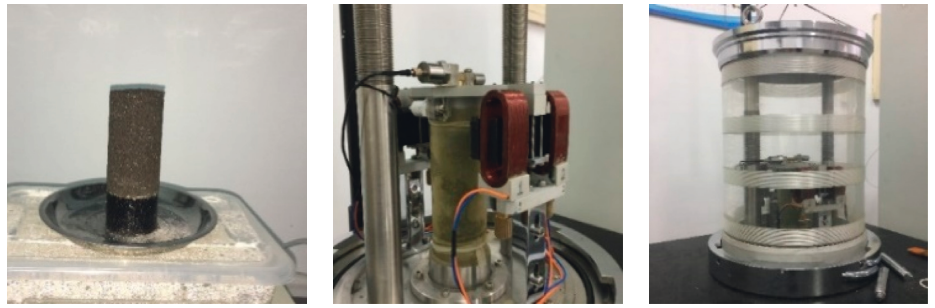

(a) (b) (c)

Figure 4: Test sample in the resonant column apparatus: (a) formed sample; (b) loading sample; (c) sample covered with the pressure chamber.

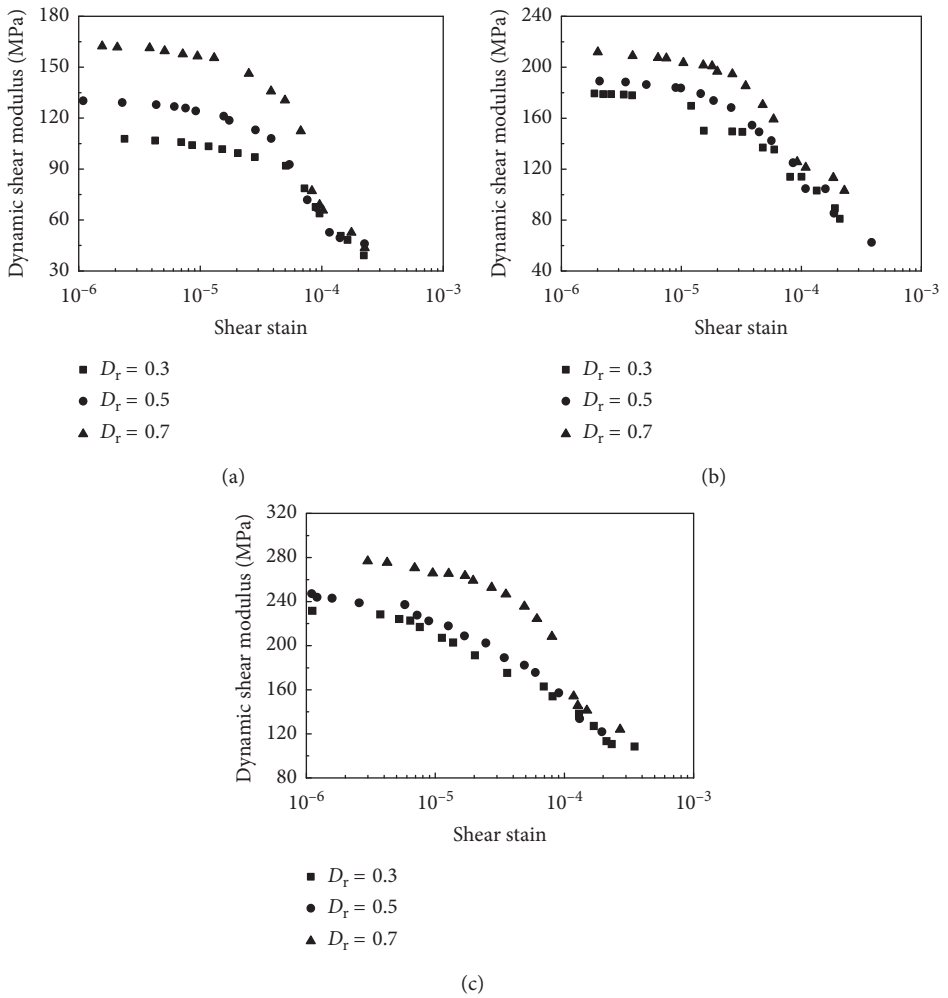

Figure 5: Effect of relative density on the G-γ curve of steel slag: (a) $\sigma = 100$ kPa; (b) $\sigma = 200$ kPa; (c) $\sigma = 300$ kPa.

when the shear strain was small and the dynamic energy loss was relatively smaller. When the shear strain of the steel slag increased, the stress wave resistance became larger and the energy consumption became large. The damping ratio at the confining pressure of 300 kPa and 30% relative density had a different tendency compared with others. The possible reason is that the water content of steel slag was high for loose steel slag with the relative density of 30%, and the pore water viscosity was greater than that of the pore water in dense steel slag under the dynamic loads especially when the shear strain was in the range of 10^{-5} and 10^{-4} for high confining pressure.

3.2. Effect of Confining Pressure. The relationships between the dynamic shear modulus and the shear strain of the steel

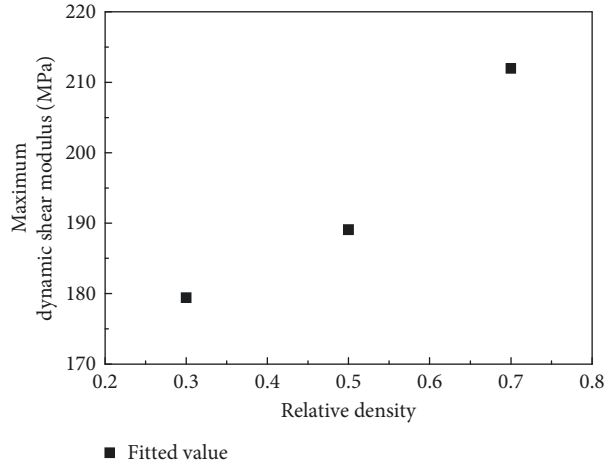

Figure 6: Relationship between the maximum dynamic shear modulus and relative density ($\sigma = 200$ kPa).

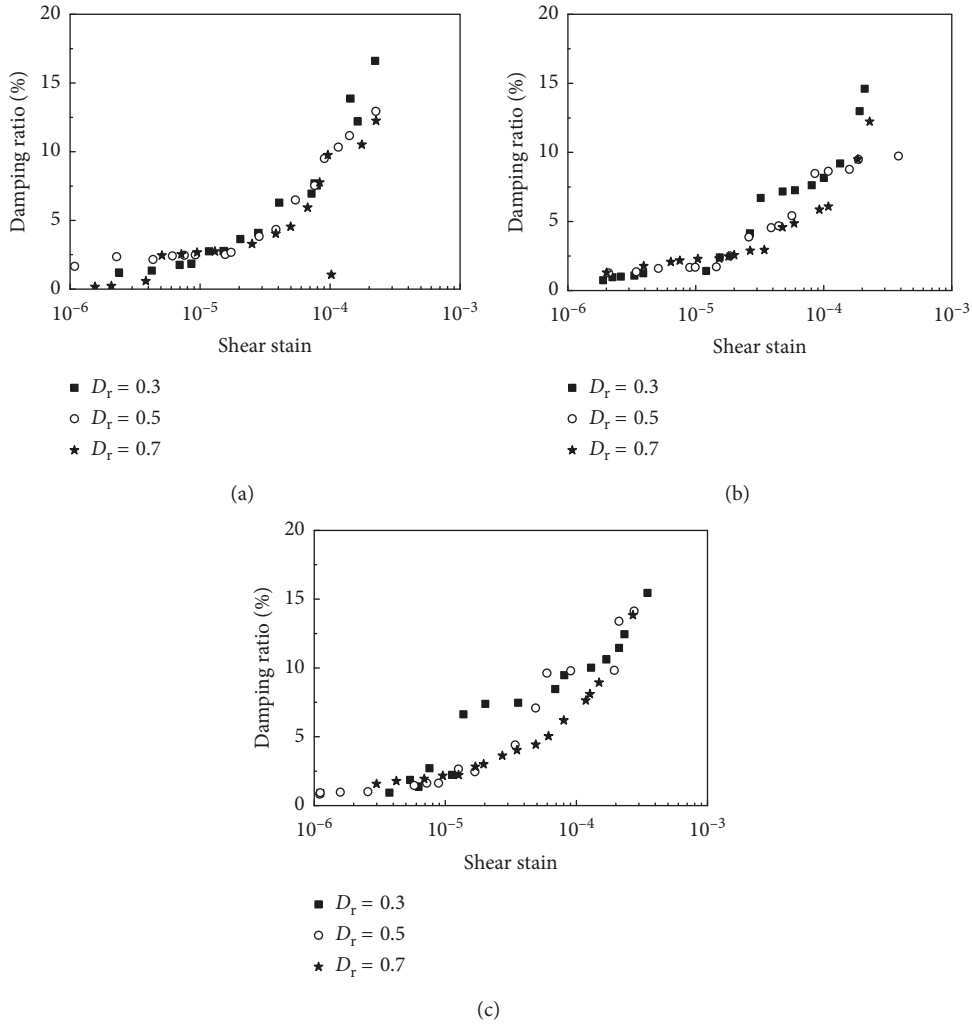

Figure 7: Effect of the damping ratio on the λ-γ curve of steel slag: (a) $\sigma = 100$ kPa; (b) $\sigma = 200$ kPa; (c) $\sigma = 300$ kPa.

slag with different confining pressures are shown in Figure 8 when the relative densities of the steel slag were, respectively, 30%, 50%, and 70%.

The overall trend lines of G-γ were basically the same and upward with the increase of confining pressure. The greater the confining pressure was, the larger the dynamic shear

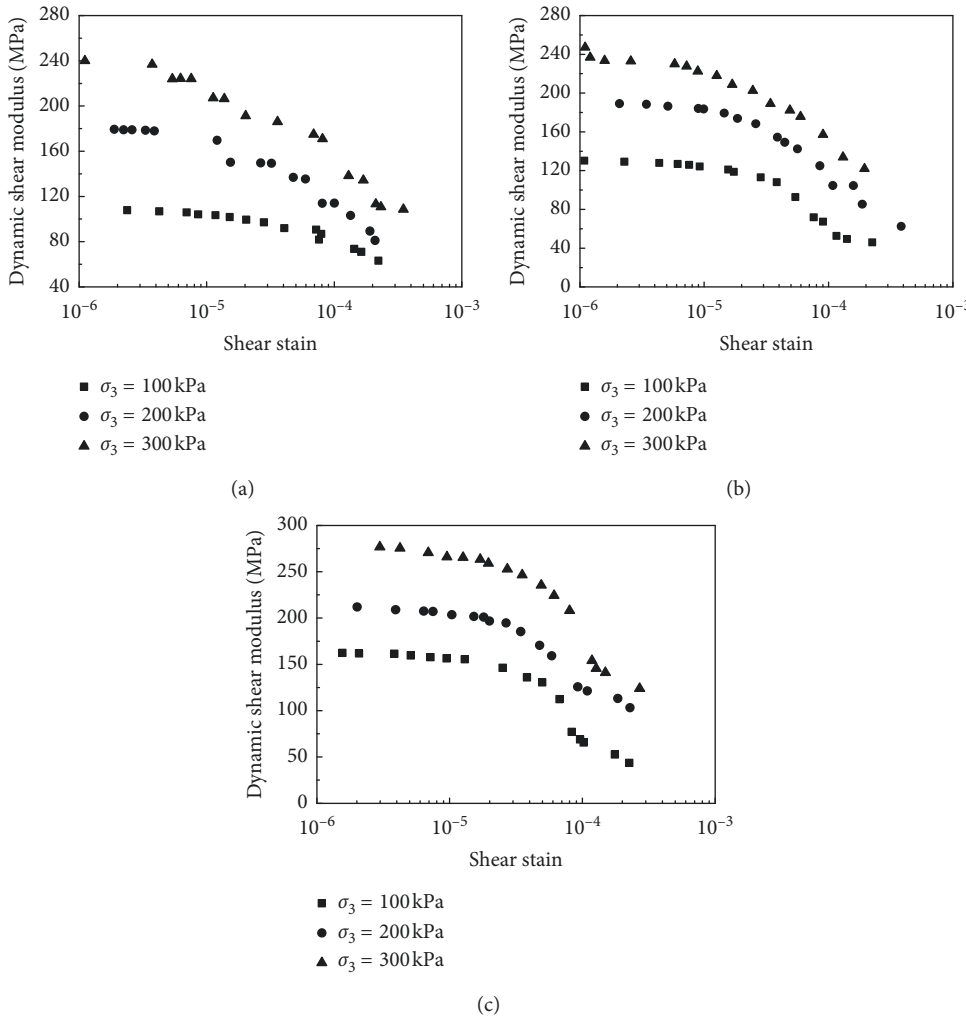

Figure 8: Effect of confining pressure on the G-γ curve of steel slag: (a) $D_r = 0.3$; (b) $D_r = 0.5$; (c) $D_r = 0.7$.

modulus was. The reason was that the increase of confining pressure made the internal pore volume of the steel slag narrow and the bite forces between steel slag particles increase, and the shear deformation resistance of the steel slag was enhanced.

3.3. Maximum Dynamic Shear Modulus. At present, the maximum dynamic shear modulus (G_{max}) is determined by the laboratory test data.

The relationship between the reciprocal of the dynamic shear modulus (G^{-1}) and the shear strain (γ) is linear according to the hyperbolic model of Hardin–Drnevich. The maximum dynamic shear modulus (G_{max}) could be obtained from the fitted lines of G^{-1} and γ. The maximum dynamic shear modulus was the intercept of the G^{-1}-γ line. The fitted lines of G^{-1} and γ are shown in Figure 9, and the fitting parameters are shown in Table 3.

With the increase of confining pressure, the overall trend of the G-1-γ lines was downward. As can be seen from Table 3, with the increase of relative density, the maximum dynamic shear modulus of the steel slag had been significantly improved. With the increase of confining pressure, the maximum dynamic shear modulus of the steel slag with different relative densities also increased. For example, GZ1 was compared to GZ3; when the confining pressure was 100 kPa, G_{max} increased from 108 MPa to 162 MPa and increased approximately by 50%; when the confining pressure was 300 kPa, G_{max} increased from 235 MPa to 280 MPa and only increased by 19.5%. This finding showed that the relative density had greater effect on the maximum dynamic shear modulus of the steel slag with low confining pressure than with high confining pressure. Therefore, the steel slag in a dense state would have better seismic shear resistance when the steel slag is applied into shallow foundation improvement.

4. Dynamic Model of the Steel Slag

There are three typical hyperbolic models including Davidenkov model, Hardin–Drnevich model, and Ramberg–Osgood model that could describe soil dynamic properties very well. Ramberg–Osgood model and Davidenkov model

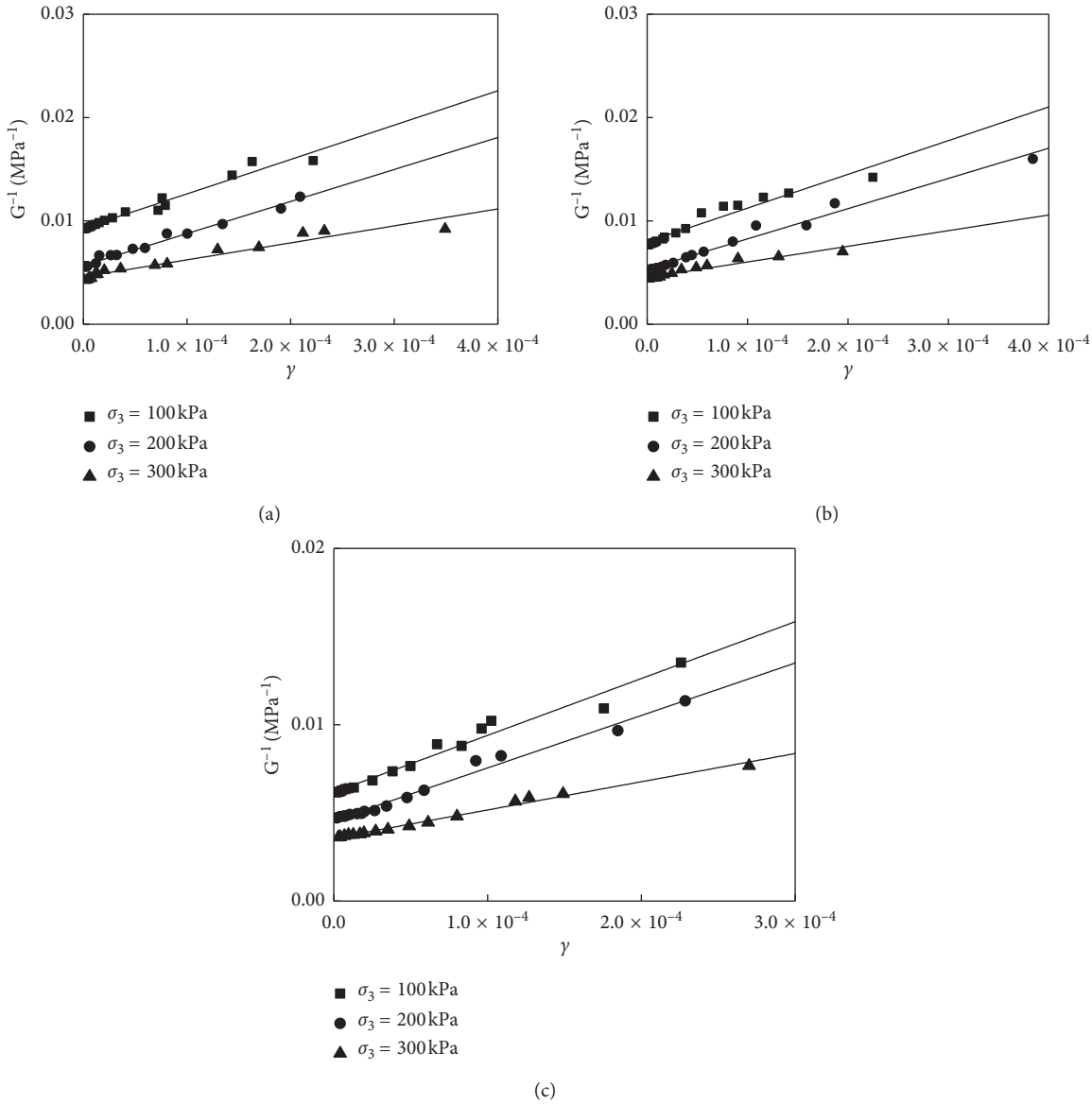

Figure 9: Fitted lines of G^{-1} and γ under different relative densities: (a) $D_r = 0.3$; (b) $D_r = 0.5$; (c) $D_r = 0.7$.

Table 3: Fitting parameters of G^{-1}.

Sample number	Relative density	Confining pressure (kPa)	B	A	G_{max} (MPa)	R^2
GZ1	30%	100	39.897	0.01115	108	0.95
		200	37.212	0.00681	176	0.97
		300	19.829	0.00512	235	0.94
GZ2	50%	100	39.172	0.00957	125	0.95
		200	35.087	0.00641	187	0.99
		300	19.283	0.00488	246	0.92
GZ3	70%	100	38.686	0.00741	162	0.95
		200	35.697	0.00549	219	0.99
		300	19.202	0.00428	280	0.98

have many experimental parameters and are usually used to fit the dynamic properties of soil under complex stress conditions. For the steel slag, the experimental parameters are less and the dynamic shear properties could be described by the Hardin–Drnevich model.

The test range of shear strain in the resonant column equipment was generally in a range of 10^{-4}~10^{-6}. The dynamic shear modulus and the damping ratio in a large strain range (larger than 5.0×10^{-4}) could be obtained by the fitting curve of the small strain dynamic model.

The relationship between the dynamic shear modulus and the shear strain was expressed as equation (3) [32], and the relationship between the damping ratio and the shear strain was expressed as equation (4):

$$\frac{G}{G_{\max}} = \frac{1}{1 + (\gamma/\gamma_r)}, \tag{3}$$

$$\frac{\lambda}{\lambda_{\max}} = \frac{(\gamma/\gamma_r)}{1 + (\gamma/\gamma_r)}, \tag{4}$$

where γ, γ_r, $G_{\max}$ and $\lambda_{\max}$ represent the dynamic shear strain, reference shear strain, maximum shear modulus, and maximum damping ratio, respectively. Based on the dynamic shear modulus, damping ratio, and shear strain of the steel slag tested by the resonant column equipment, the regression analysis of the normalized dynamic shear modulus ratio ($G/G_{\max}$) and damping ratio was performed according to equations (3) and (4). The fitting results are listed in Figure 10 and in Table 4. As could be seen from Table 4, with the increase of the relative density and confining pressure, the maximum dynamic shear modulus of the steel slag increased. It showed that the reference shear strain could be improved by increasing the relative density and confining pressure.

Figure 10 showed that, with the increase of the confining pressure, the fitting curves of $G/G_{\max}$-γ moved upward and the fitting curves of λ-γ moved downward, but not obvious. Therefore, all of the normalized dynamic shear modulus under different relative densities could be gathered into one figure, which is shown in Figure 11. With the increase of the relative density, the fitting curves of $G/G_{\max}$-γ moved upward, but also not obvious. Three fitting curves were close together, and the fitting effect was great, showing that it was appropriate to use equations (3) and (4) to fit the normalized dynamic shear modulus and the damping ratio of the steel slag.

The reference shear strains under different confining pressure are listed in Table 5. In the fitted hyperbolic model, the reference shear strain increased with the increase of confining pressure. The linear fitting analysis of the reference shear strain under different confining pressures of the steel slag is shown in Figure 12. The linear fitting equation is shown in equation (5). The results showed that the linear fitting effect was perfect between the reference shear strain and confining pressure:

$$\gamma_r = 2.09 \times 10^{-7} \cdot \sigma_3 + 1.28 \times 10^{-4}. \tag{5}$$

Considering the influence of confining pressures and combing equations (3) and (5), the Hardin–Drnevich model of the steel slag dynamic properties was established. The dynamic model is shown in the following equation:

$$\frac{G}{G_{\max}} = \frac{1}{1 + \left(\gamma/2.09 \times 10^{-7} \cdot \sigma_3 + 1.28 \times 10^{-4}\right)}. \tag{6}$$

The test range of the steel slag shear strain in the resonant column equipment was in a range of 10^{-4}~10^{-6}. The dynamic shear modulus and the damping ratio of the steel slag in a large strain range (larger than 5.0×10^{-4}) would be obtained by the dynamic triaxial test.

5. Comparisons of Dynamic Shear Modulus with Sand

To understand the shear resistance of the steel slag under dynamic loading, the maximum dynamic shear modulus of the steel slag was compared with those of Nanjing fine sand and Fujian standard sand. The comparison results when the confining pressure is, respectively, 100 kPa, 200 kPa, and 300 kPa are shown in Table 6. In this instance, $G_{\max}$ represents fitted values. Figure 13 is the comparison of the maximum dynamic shear modulus for three materials. The maximum dynamic shear modulus data of Nanjing fine sand when the confining pressure was 300 kPa were lacking [33].

The maximum dynamic shear modulus of the steel slag was far greater than Nanjing fine sand no matter what the confining pressure was. Furthermore, the maximum dynamic shear modulus of steel slag was similar to that of Fujian sand in the manuscript except for low confining pressure. The maximum dynamic shear modulus of waste steel slag was close to Fujian sand under low confining pressure. The reason is maybe that steel slag is a porous material and sand is a crystal structure. Porosity character of steel slag is obvious under low confining pressure and dynamic loads. Especially, when the confining pressure was high and reached 300 kPa, the maximum dynamic shear modulus of the steel slag was in the range of those of Fujian standard sand. Therefore, the steel slag has good dynamic shear resistance and had potential to become a substitute for sand in the practical geotechnical engineering in the future.

6. Conclusion

The dynamic shear characteristics of the steel slag were initially studied by resonance column tests, and the following conclusions were obtained:

(1) The dynamic shear modulus of the steel slag decreased with the increase of shear strain, and the damping ratio increased with the increase of shear strain. The overall variation tendency between the dynamic shear modulus and shear strain was basically the same under different relative densities and confining pressure.

(2) The greater the relative density of the steel slag was, the larger the dynamic shear modulus of the steel slag was. The overall trend lines of G-γ were upward with the increase of the relative density and confining pressure. The confining pressure and relative density had remarkable influence in a small strain range on the dynamic shear modulus of the steel slag.

(3) The maximum dynamic shear modulus of the steel slag had a good linear relationship with the relative density of the steel slag. With the increase of the relative density and confining pressure, the

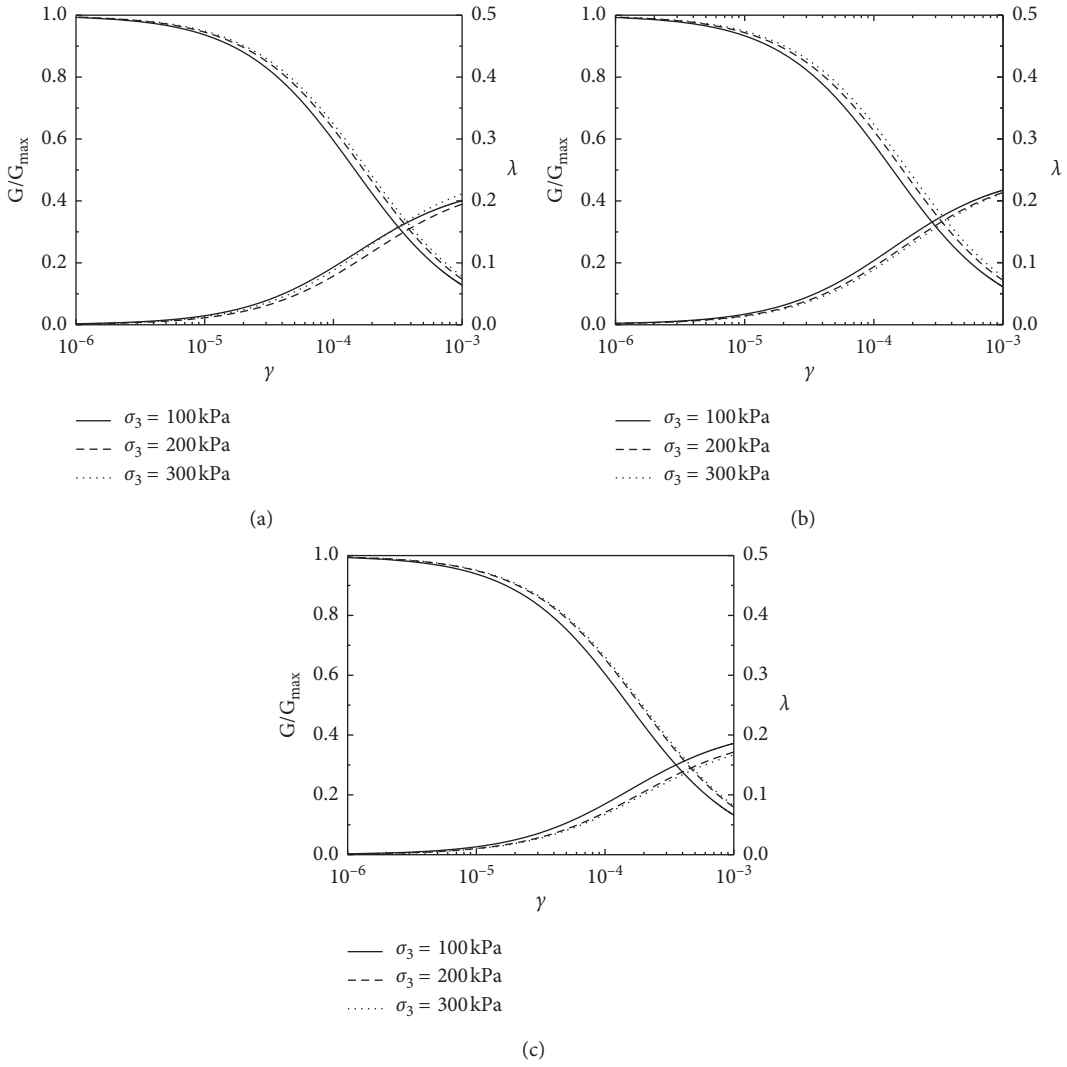

Figure 10: Fitted curves of G/G_{max}-γ and λ-γ under different mixing ratios: (a) $D_r = 0.3$; (b) $D_r = 0.5$; (c) $D_r = 0.7$.

Table 4: Fitting results of test parameters.

Sample number	Relative density	Confining pressure (kPa)	G_{max} (MPa)	λ_{max} (%)	γ_r	R^2
GZ1	30%	100	108	0.247	1.39×10^{-4}	0.98
		200	176	0.249	1.67×10^{-4}	0.98
		300	235	0.251	1.84×10^{-4}	0.93
GZ2	50%	100	125	0.229	1.47×10^{-4}	0.98
		200	187	0.186	1.72×10^{-4}	0.97
		300	246	0.223	1.94×10^{-4}	0.90
GZ3	70%	100	162	0.214	1.53×10^{-4}	0.97
		200	219	0.204	1.89×10^{-4}	0.96
		300	280	0.200	1.96×10^{-4}	0.95

maximum dynamic shear modulus of the steel slag increased.

(4) The regression analysis of the normalized dynamic shear modulus ratio and damping ratio was performed very well according to the Hardin–Drnevich model. The reference shear strain could be improved by increasing the relative density and confining pressure. The linear fitting effect was perfect between the reference shear strain and confining pressures.

(5) The dynamic shear modulus of the steel slag was far greater than Nanjing fine sand no matter what the confining pressure was and was similar to those of Fujian standard sand. Especially when the confining

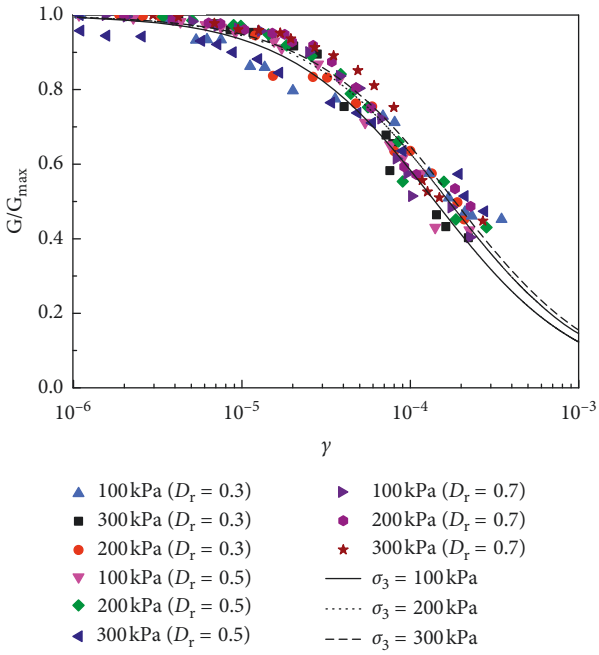

Figure 11: Fitted curves of G/G_{max}-γ under different confining pressures.

Table 5: Reference shear strains under different confining pressures.

Sample number	Confining pressure	Reference shear strain
GZ1	30%	1.47×10^{-4}
GZ2	50%	1.76×10^{-4}
GZ3	70%	1.88×10^{-4}

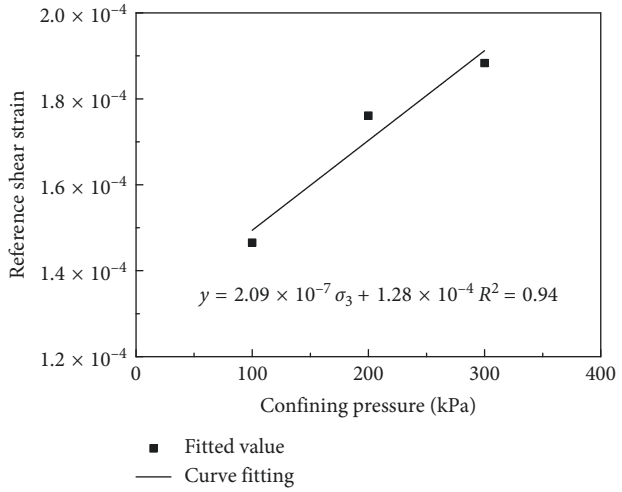

Figure 12: Fitted curves between reference shear strain and confining pressure.

pressure reached 300 kPa, the maximum dynamic shear modulus of the steel slag was in the numerical range of those of Fujian standard sand. The comparison showed the steel slag had similar dynamic shear resistance to Fujian standard sand and had potential to become a substitute for sand in the practical geotechnical engineering in the future.

Table 6: Comparisons of G_{max} for steel slag, fine sand, and standard sand.

Confining pressure (kPa)	G_{max} (MPa)		
	100	200	300
Nanjing fine sand [33]	47~54	66~74	\
Fujian standard sand [32]	126~197	174~272	211~323
Steel slag	108~125	162~219	235~280

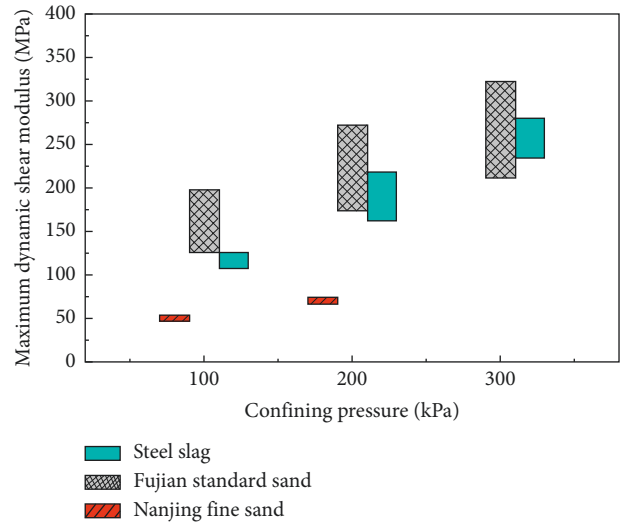

Figure 13: Comparison of the maximum dynamic shear modulus of steel slag with traditional sands.

Data Availability

The data used to support the findings of this study are available from the corresponding author upon request.

Conflicts of Interest

The authors declare that they have no conflicts of interest.

Acknowledgments

This research was financially supported by the Natural Science Foundation of Jiangsu Province (Grant no. BK20161360), the Six Major Talents Peak in Jiangsu Province in China (Grant no. 2016-JZ-020), and Postgraduate Research and Practice Innovation Program of Jiangsu Province (Grant no. SJCX17_0609).

References

[1] Y. Huang, R. N. Bird, and O. Heidrich, "A review of the use of recycled solid waste materials in asphalt pavements," *Resources, Conservation and Recycling*, vol. 52, no. 1, pp. 58–73, 2007.

[2] W.-T. Tsai, "Analysis of the sustainability of reusing industrial wastes as energy source in the industrial sector of Taiwan," *Journal of Cleaner Production*, vol. 18, no. 14, pp. 1440–1445, 2010.

[3] T. Huang, X. Z. Wang, Y. G. Wu et al., "Experimental research and application of Yubei steel slag pile composite foundation," *Chinese Journal of geotechnical engineering*, vol. 21, no. 3, pp. 72–77, 1999.

[4] Z. H. Liao, *Guide to Application of New Materials in Highway Engineering*, China Communications Press, Beijing, China, 2004.

[5] C. Yan, S. Y. Liu, and Y. F. Deng, "Experimental research for the application of mining waste in the trench cutting remixing deep wall method," *Advances in Materials Science and Engineering*, vol. 2015, Article ID 202848, 9 pages, 2015.

[6] M. Z. Hu, "The application of steel slag in Lou-Lian highway," *Highway and Car Transport*, vol. 10, no. 2, pp. 52-53, 2006, in Chinese.

[7] W. Li, H. L. Wang, Li F. Li et al., "Mechanical property tests of mixed soil materials of waste steel slag and sand," *Journal of Shenyang Construction University (NATURAL SCIENCE EDITION)*, vol. 16, no. 5, pp. 794–799, 2008.

[8] L. Y. Wang, P. Gao, and G. X. Chen, "Experimental studies on the compressive deformation and strength characteristics of new mixed lightweight sand blended with waste steel slag," *Chinese Journal of Geotechnical Engineering*, no. S2, pp. 204–209, 2013, in Chinese.

[9] S. Shulin, J. Tang, and Q. H. Zheng, "Experimental study of expansive soil improved with granulated blast furnace slag (GBFS)," *Rock and Soil Mechanics*, vol. 33, no. 7, pp. 1940–1944, 2012.

[10] A. E. brahim and A. E.-M. Behiry, "Evaluation of steel slag and crushed limestone mixtures as subbase material in flexible pavement," *Ain Shams Engineering Journal*, vol. 4, no. 1, pp. 44–53, 2013.

[11] Y. Laxmikant and R. K. Tripathi, "Effect of the length of geogrid layers in the bearing capacity ratio of geogrid reinforced granular fill-soft subgrade soil system," *Procedia—Social and Behavioral Sciences*, vol. 104, pp. 225–234, 2013.

[12] Y.-N. Sheen, L.-J. Huang, H.-Y. Wang, and D.-C. Le, "Experimental study and strength formulation of soil-based controlled low-strength material containing stainless steel reducing slag," *Construction and Building Materials*, vol. 54, pp. 1–9, 2014.

[13] Y. Chao, L. Songyu, and D. Yongfeng, "Experimental research for the application of mining waste in the trench cutting remixing deep wall method," *Advances in Materials Science and Engineering*, pp. 1–9, 2015.

[14] M. Shahbazi, M. Rowshanzamir, S. M. Abtahi, and S. M. Hejazi, "Optimization of carpet waste fibers and steel slag particles to reinforce expansive soil using response surface methodology," *Applied Clay Science*, vol. 142, pp. 185–192, 2017.

[15] L. Y. Wang, J. T. Yan, Q. Wang, B. H. Wang, and A. Ishimwe, "Study on permeability of steel slag and steel slag modifying silt soil as new geo-backfill materials," *Advances in Civil Engineering*, vol. 2018, 2018, In press.

[16] G. X. Chen, X. Z. Liu, D. H. Zhu et al., "Experimental studies on dynamic shear modulus ratio and damping ratio of recently deposited soils in Nanjing," *Chinese Journal of Geotechnical Engineering*, vol. 28, no. 8, pp. 1023–1027, 2006.

[17] G. Chen, Z. Zhou, T. Sun et al., "Shear modulus and damping ratio of sand–gravel mixtures over a wide strain range," *Journal of Earthquake Engineering*, vol. 2017, no. 10, 2017.

[18] X. Z. Ling, F. Zhang, Q. L. Li, L. S. An, and J. H. Wang, "Dynamic shear modulus and damping ratio of frozen compacted sand subjected to freeze-thaw cycle under multistage cyclic loading," *Soil Dynamics and Earthquake Engineering*, vol. 76, pp. 111–121, 2015.

[19] P. H. H. Giang, P. O. V. Impe, W. F. V. Impe, P. Menge, and W. Haegeman, "Small-strain shear modulus of calcareous sand and its dependence on particle characteristics and gradation," *Soil Dynamics and Earthquake Engineering*, vol. 100, pp. 371–379, 2017.

[20] K. Senetakis, A. Anastasiadis, and K. Pitilakis, "Dynamic properties of dry sand/rubber (SRM) and gravel/rubber (GRM) mixtures in a wide range of shearing strain amplitudes," *Soil Dynamics and Earthquake Engineering*, vol. 33, no. 1, pp. 38–53, 2012.

[21] W. Zhou, Y. Chen, G. Ma, L. Yang, and X. Chang, "A modified dynamic shear modulus model for rockfill materials under a wide range of shear strain amplitudes," *Soil Dynamics and Earthquake Engineering*, vol. 92, pp. 229–238, 2017.

[22] H. Zhuang, R. Wang, G. Chen, Y. Miao, and K. Zhao, "Shear modulus reduction of saturated sand under large liquefaction-induced deformation in cyclic torsional shear tests," *Engineering Geology*, vol. 240, pp. 110–122, 2018.

[23] L.-Y. Wang, H.-L. Liu, P.-M. Jiang, and X.-X. Chen, "Prediction method of seismic residual deformation of caisson quay wall in liquefied foundation," *China Ocean Engineering*, vol. 25, no. 1, pp. 45–58, 2011.

[24] L. Y. Chen, S. K. Chen, and P. Gao, "Research on seismic internal forces of geogrids in reinforced soil retaining wall structures under earthquake actions," *Journal of Vibroengineering*, vol. 16, no. 4, pp. 2023–2034, 2014.

[25] L. Wang, G. Chen, and S. Chen, "Experimental study on seismic response of geogrid reinforced rigid retaining walls with saturated backfill sand," *Geotextiles and Geomembranes*, vol. 43, no. 1, pp. 35–45, 2015.

[26] L. Y. Wang, G. X. Chen, P. Gao et al., "Pseudo-static calculation method of the seismic residual deformation of a geogrid reinforced soil retaining wall with a liquefied backfill," *Journal of Vibroengineering*, vol. 17, no. 2, pp. 827–840, 2015.

[27] G. Q. Kong, L. D. Zhou, Z. T. Wang, G. Yang, and H. Li, "Shear modulus and damping ratios of transparent soil manufactured by fused quartz," *Materials Letters*, vol. 182, pp. 257–259, 2016.

[28] W.-x. Gong, L.-y. Wang, J. Li, and B.-h. Wang, "Displacement calculation method on front wall of covered sheet-pile wharf," *Advances in Civil Engineering*, vol. 2018, Article ID 5037057, 13 pages, 2018.

[29] Y. Chuancheng, C. Wenxia, and D. Haiyue, "Research on comparison of the maximum dynamic shear modulus test," *Procedia Engineering*, vol. 28, pp. 230–234, 2012.

[30] L. Y. Wang, X. T. Cao, Q. Wang, and B. H. Wang, "Dynamic properties of steel slag improved with sand-tire shreds admixture," *Proceedings of the Institution of Civil Engineers—Ground Improvement*, vol. 2018, pp. 1–17, 2018.

[31] L. Y. Wang, B. T. Huang, and P. Gao, "A new geo-material consisting of industrial wastes and its preparation and application," China, No. Patent: ZL20131 0186058, 2013.

[32] X. M. Yuan and J. Sun, "Model of maximum dynamic shear modulus of sand under anisotropic consolidation and revision of Hardin's formula," *Chinese Journal of Geotechnical Engineering*, vol. 3, pp. 264–269, 2005.

[33] B. H. Wang, G. X. Chen, and Q. X. Hu, "Experiment of dynamic shear modulus and damping of Nanjing fine sand," *World Earthquake Engineering*, vol. 26, no. 9, pp. 7–15, 2010.